2022 EAGE ANNUAL
83RD CONFERENCE & EXHIBITION
MADRID I SPAIN

FULL WAVEFORM INVERSION WITH LOW FREQUENCY RECONSTRUCTED DATA

R. Djebbi[1], M. Bekara[1], N. Chemingui[1], J. Ramos-Martinez[1], A. Asnaashari[1]

[1] PGS

Summary

Full Waveform Inversion (FWI) requires the minimization of a highly non-linear objective function which makes the inversion suffer from cycle-skipping. To overcome this issue, we need to have an accurate initial velocity model and/or input seismic data with good low-frequency content. However, low frequencies can be very noisy, and conventional noise attenuation tools fail to recover the useful signal. In this abstract, we propose to apply a novel low-frequency reconstruction method to condition the data for Full Waveform Inversion. The reconstruction is done from the higher frequencies using a recursive filter which is estimated from the data itself. We apply the low-frequency reconstruction method on synthetic data to show its high accuracy even in presence of strong noise extracted from field data. We successfully performed FWI using low frequency reconstructed field data starting from simple velocity models. The reconstructed low frequencies help to mitigate the cycle-skipping observed when these frequencies cannot be utilized in the inversion and the initial models are not accurate. Results demonstrate the effectiveness of the novel data reconstruction method and show its benefits in reducing the turnaround time for building accurate velocity models by FWI, when starting from less suitable initial velocity models.

Full Waveform Inversion with low frequency reconstructed data

Introduction

Full waveform inversion (FWI) is based on the minimization of the misfit error measured between the field data and the numerically modelled data using an approximate earth model (Tarantola, 1984). As the cost function is highly nonlinear, FWI can suffer from convergence to local minima, known also as cycle-skipping. This leads to an incorrect inverted model and undermine the use of FWI.

Many strategies have been proposed in the literature to deal with this problem. Luo and Schuster (1991) proposed using the time-lag as an alternative objective function to reduce the nonlinearity of the FWI problem. Choi and Alkhalifah (2013) used the phase derivative which can unwrap the phase and improve the convergence to the global minimum. Extended domain FWI (Symes, 2008) is another class of methods, where an extension in the model or the data domains improves the convexity of the objective function. Huang et al. (2021) proposed a FWI objective function using time-warping extension. The problem is solved in a single objective function using the Alternate Direction Method (ADM) and was successfully applied to field data with poor low-frequency content.

Despite the progress in improving the convexity of the objective function in FWI, low frequencies are still vital to mitigate the cycle-skipping problem and at the same time, to better reconstruct the background velocity model, particularly in complex geological settings. Noise attenuation is routinely used to enhance the signal-to-noise ratio (SNR) at low frequencies. However, this solution fails when the input SNR is very poor. As an alternative, a lot of efforts have been put to reconstruct the useful low frequencies using methods that range from signal processing (Li and Demanet, 2016) to machine learning techniques (Ovcharenko et al., 2017).

In this abstract, we show the results of applying our recently developed method for Low Frequency Reconstruction (LFR) to improve the FWI results (Bekara et al., 2022). The method is applied on both synthetic and field datasets and demonstrates a clear advantage in helping FWI to minimize cycle-skipping. We briefly describe the LFR approach and the FWI algorithm, then we show the low-frequency reconstruction and FWI applications results.

Method

The reconstruction is carried out from the higher frequencies using a recursive filter which is estimated from the data itself. The method transforms the data locally, over sliding data windows, from the time-space domain to the frequency-slowness domain where the reconstruction is performed. The data transformation is important to enforce the sparsity assumption of the signal, include the spatial correlation in the data and honour the constraint of the "signal cone" of the wavefield. In addition, the reconstruction is done stepwise, i.e., a frequency sample is reconstructed at each step with a re-estimation of the recursion model (Bekara et al., 2022).

To demonstrate the benefits of the reconstruction of the low frequencies in FWI, we use an inversion algorithm based on the conventional $\boldsymbol{L_2}$ objective function formulated as follows:

$$J[m] = \frac{1}{2}||F[m] - d||_2^2 \ , \qquad (1)$$

where m is the velocity model, $F[m]$ is the synthetic data and d is the field data.

We apply a multiscale approach starting from the lowest available frequencies to achieve optimal convergence to the right model. Because reflections in addition to refractions are used in the inversion, at the initial inversion stages, we use the gradient kernel proposed by Ramos-Martinez et al., (2016), which enhances the long wavelengths and removes the high wavenumber migration isochrones. We show FWI results on the synthetic Marmousi II model and two field datasets from offshore Malaysia and Angola.

Synthetic example

For this synthetic example, the source/receiver geometry mimics a typical streamer acquisition with a maximum offset of 8 km. The source wavelet is a Ricker wavelet with 16 Hz peak frequency. Figure 1-a shows the modelled data (noise free) in the 1-4 Hz frequency band. In Figure 1-b, we add low-frequency noise extracted from field data. The noise is very strong and the SNR equals -46dB at 2 Hz,

and -18dB at 4 Hz which makes conventional denoising processes ineffective. Figure 1-c shows the result of the application of a sequence of F-X projection and F-X prediction filters in various data sorting domains. The LFR result is shown in Figure 1-d. Frequencies below 4 Hz are reconstructed using higher frequencies (4-8 Hz). The quality of the data is considerably improved and most of the events are recovered with high accuracy.

We run two multi-stage FWI tests for denoised and LFR data up to 16 Hz (1-4 Hz; 2-6 Hz; 2-8 Hz; 2-12 Hz; 2-16 Hz). For the denoised data the first stage is ignored, and the inversion starts with 2-6 Hz frequency band. The initial model for both tests is a heavily smoothed version of the true model. With this model, FWI from the conventionally denoised data converges to a local minimum as shown in Figure 2-c. In contrast, the LFR data enables FWI to start at a frequency band in which there is no cycle-skipping. Therefore, the inversion converges to a nearly perfect model (Figure 2-d).

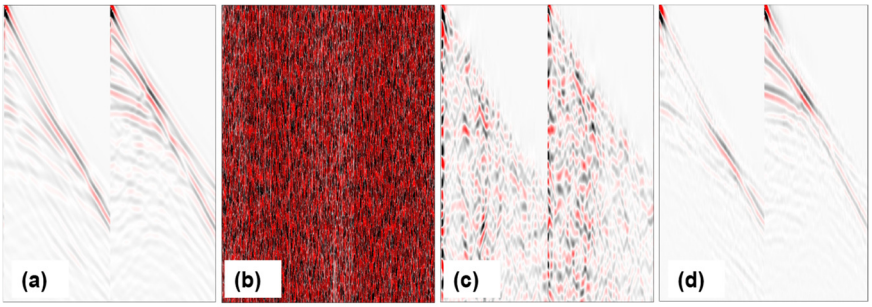

Figure 1 *Marmousi II synthetic example. Input shot gathers for a 1 to 4Hz frequency bandwidth. (a) Noise-free gathers; (b) gathers with added actual field data noise; (c) gathers after conventional denoising; (d) gathers after applying LFR.*

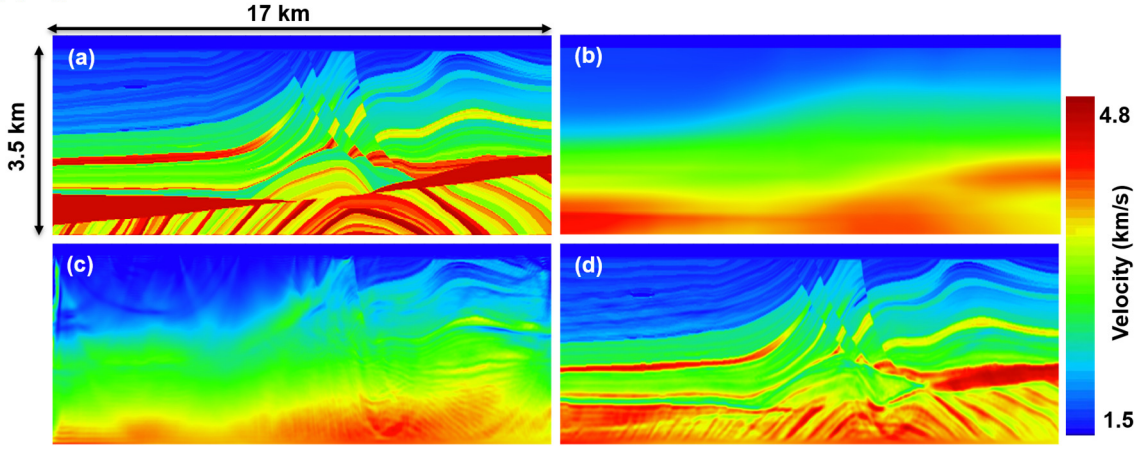

Figure 2 *Marmousi II synthetic example. (a) True, (b) initial, and inverted models using data with (c) conventional denoising and (d) LFR.*

Field data examples

We applied the proposed LFR method to enhance the low-frequency content of field seismic data, as an alternative data conditioning to conventional denoising for FWI applications. The first dataset corresponds to a towed-streamer line acquired offshore Malaysia using the continuous wavefields method (Klüver et al., 2020). Data were acquired utilizing multi-sensor technology with a maximum inline offset of 8.1 km. We perform two FWI tests with and without low-frequency reconstruction (< 4Hz). The initial velocity model is a constant gradient model which produces clear cycle-skipping even at intermediate offsets as observed in the comparison of field and modelled data (Figure 3-c). Also, it is evident that the initial velocity field requires positive updates in the shallow part of the model. For the LFR data, we performed FWI in a multi-stage fashion up to 16 Hz (at stages of 1-2 Hz, 1-3 Hz, 2-4 Hz, 2-6 Hz, 2-8 Hz, 2-12 Hz and 2-16 Hz). For the test without LFR data, the first three stages were not possible because of the poor SNR at those frequency bandwidths. The final FWI results are shown in Figures 3-a and 3-b and there is a clear difference between the two models. We carried out modelling to assess the two solutions. After FWI with no LFR, the slow-down in the shallow part of the model moved the modelled data to the wrong direction (Figure 3-d). In contrast, the synthetic data computed with the FWI model obtained from LFR data, matches very well the field data as shown in Figure 3-e. We also performed migration and computed the angle gathers from both final models to further evaluate the results. Migrated stack computed from the FWI model using LFR data (Figure 4-b) shows a better

reflector continuity and energy focusing compared to that obtained from the FWI model with no LRF data (Figure 4-a). This is validated by comparing the gather flatness for both models (Figures 4-c and 4-d).

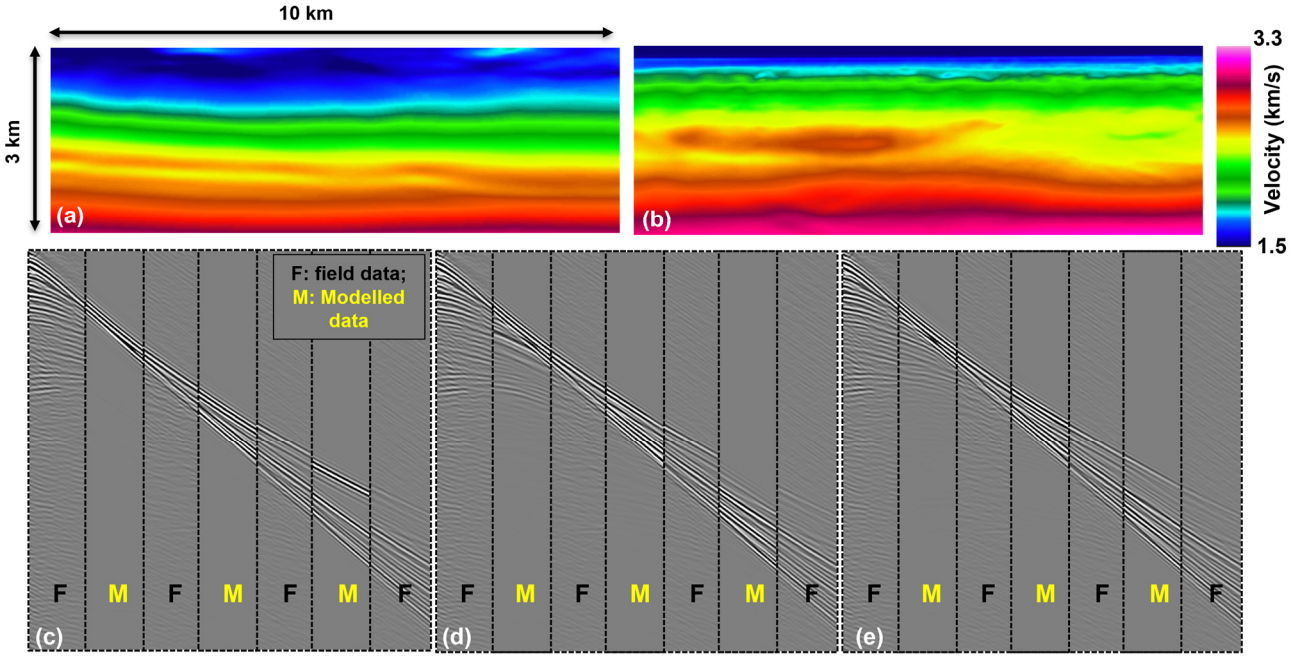

Figure 3 *Malaysia field data example. FWI models (a) without and (b) with LFR. Comparison of field and modelled data from the (c) initial and the FWI models (d) without and (e) with LFR. Offset panels for field and modelled data are labelled with F and M, respectively.*

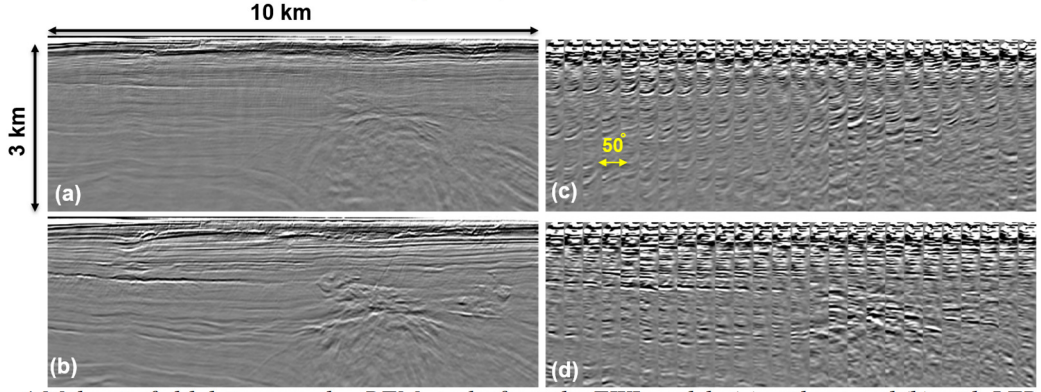

Figure 4 *Malaysia field data example. RTM stacks from the FWI models (a) without and (b) with LFR. RTM angle gathers from the FWI models (c) without and (d) with LFR.*

The second field data example corresponds to multi-sensor data acquired in offshore Angola. The original data is only cycle-skipped in a small part of the model shown by the black ellipses in Figure 5-a, 5-b. Synthetic data computed from the initial model (Figure 5-c) for the shot located on top of this area (Shot 1), shows poor data fitting at mid-offsets and stronger mismatch at far-offsets, where the cycle-skipping is evident. We show in Figure 5-a and 5-b the FWI updates without and with LFR, respectively. The updates are similar in most areas except at the area highlighted by the black ellipses. The LFR of data changed the direction of the FWI updates overcoming the cycle-skipping issue caused by the inaccuracy of initial model in this area. This is validated by the shot modelling from both FWI models (Figure 5-d, 5-e). Improvement in the waveform fitting from the FWI with LFR data is clearly observed in Shot 1. It is noted that the modelling (Shot 2) and results of FWI with and without LFR are similar for the area where there is no cycle-skipping. This illustrates that there is no harm to use LFR data even when the initial model is already accurate enough for starting FWI.

Conclusions

We have successfully applied a novel method to reconstruct the low-frequency content of seismic data used for FWI. The reconstruction solution is easy to deploy in production, computationally efficient and

does not require customized offline training as it is the case for similar solutions. The uplift of using the proposed solution for FWI applications is shown through data and image domain QCs of the results and confirms its ability for mitigating the cycle-skipping problem. This solution allows to relax the initial model requirements imposed by FWI and therefore leads to a reduction in the turnaround time to build high resolution models.

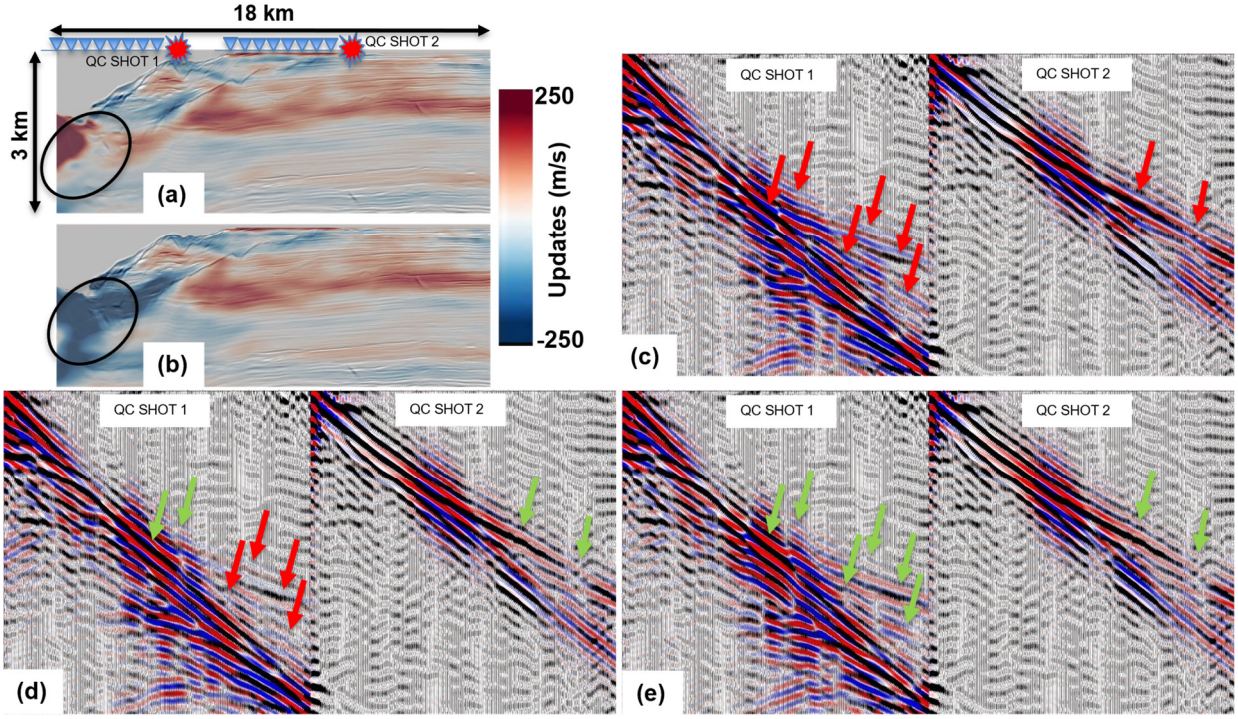

Figure 5 *Angola field data example. FWI updates (12 Hz) using data without (a) and with (b) LFR. Modelled data (colour scale) overlaying the field records (wiggle display) computed from the initial (c), FWI without LFR (d) and FWI with LFR (e). In the shot gather comparison, red (colour scale) and white (wiggle display) corresponds to negative polarities.*

Acknowledgements

We would like to thank Tilman Klüver, Stian Hegna and Guanghui Huang for their help with Malaysia dataset. Courtesy to Eni for the Angola dataset and to PGS for authorizing the publication of this material.

References

Bekara, M., Djebbi R., and Chemingui N. [2022] A new look at autoregressive low frequency reconstruction of seismic data. *Submitted to 83rd EAGE Conference & Exhibition, Extended Abstracts.*

Choi, Y. and Alkhalifah T. [2013] Frequency-domain waveform inversion using the phase derivative. *Geophysical Journal International*, **195**, 1904-1916.

Huang, G., Ramos-Martínez, J., Yang, Y., Djebbi, R. and Chemingui, N. [2021] Extended domain FWI via time warping. *82nd EAGE Annual Conference & Exhibition, Extended Abstracts.*

Klüver, T., Hegna, S., and Lima, J. [2020] Continuous wavefields method: Insights from a shallow water field trial. *90th SEG meeting, SEG Expanded Abstracts.*

Li, Y. E., and Demanet, L. [2016] Full-waveform inversion with extrapolated low-frequency data. *Geophysics*, **81**, R339-R348.

Luo, Y. and Schuster, G.T. [1991] Wave-equation traveltime inversion. *Geophysics*, **56**(5), 645-653.

Ovcharenko, O., Kazei, V., Peter, D. and Alkhalifah, T. [2017] Neural network based low-frequency data extrapolation. *In 3rd SEG FWI workshop: What are we getting.*

Ramos-Martinez, J., Crawley, S., Zou, K., Valenciano A. A., Qiu L. and Chemingui N. [2016] A robust gradient for long wavelength FWI updates. *78th EAGE Conference & Exhibition, Extended Abstracts.*

Symes, W.W. [2008] Migration velocity analysis and waveform inversion. *Geophysical Prospecting*, **56**(6), 765-790.

Tarantola, A. [1984] Inversion of seismic reflection data in the acoustic approximation. *Geophysics*, **49**,1259-1266.